A Mathematical Model of Pulse Plating on a Rotating Disk Electrode

A galvanostatic pulse plating model is presented for the electrodeposition of an alloy on a rotating disk electrode. This model is used to simulate the electrodeposition of nickel/chrome alloys. The mass transport equations used in the model include the effects of diffusion, migration and convection; and the electrode kinetics are described by the Butler-Volmer equation. It is predicted that the effect of ionic migration is significant and therefore should be included in models of pulse plating.

Ken-Ming Yin
Ralph E. White
Chemical Engineering Department
Texas A&M University
College Station, TX 77843

Introduction

Metal deposition by pulse electrolysis has received much attention in recent years. One reason for this is because the pulse current (i_p), the pulse time (T_{on}), and the relaxation time (T_{off}) can be adjusted to control the deposition process. The high pulse current during T_{on} may induce a larger electrode potential which in turn changes the relative deposition rates of different species in the case of alloy electrodeposition. Reactants depleted during T_{on} are replenished by mass transfer during T_{off}. Several mathematical approaches have been developed for the study of the mass transport and electrode kinetics of pulse plating of metals; unfortunately, most of these are for a single metal and do not apply to alloy plating. These theoretical treatments of pulse electrolysis can be classified as:

1. Analytical solutions obtained by assuming an initial stationary concentration profile and then superimposing on that a time-dependent pulsating concentration profile
2. More complete models which do not include the effects of ionic migration but must be solved by numerical methods

For the analytical solutions case, the pioneering work was done by Rosebrugh and Miller (1910). They solved analytically for the concentration profiles for several different applied current waves (constant, square, and sinusoidal) by an infinite Fourier series technique. Cheh (1971) picked Rosebrugh and Miller's solution for the square wave and used it to determine the pulse-limiting current density i_{pg}. He did this by setting the interface reactant concentration equal to zero at the end of a pulse and then solved for i_{pg}. He found that the overall time-averaged value of i_{pg} can never exceed the limiting direct current density (i_{lim}) under the same hydrodynamic conditions. These models provide analytical tools that are useful for a single electrode reaction with a single reactant. No rate expressions with kinetic parameters are included in their models. Chin (1983) proposed a comprehensive analytical treatment for a general square pulse current. He presented an infinite power series solution for the convective-diffusion equation for the rotating disk electrode. Using the same procedure as Cheh, Chin also backed out i_{pg}. In the model, he evaluated the concentration overpotential and ohmic drop by using the Nernst equation and Ohm's law. His approach can be applied to any form of square pulse, but it is limited to a single reaction.

Ibl et al. (1978, 1980) proposed a simplified picture of the pulse process by assuming a dynamic inner diffusion layer that pulsates with the frequency of the pulse current density and a stationary outer diffusion layer. He named this model the linear duplex diffusion model. This approach has been shown to be reasonably accurate (Datta and Landolt, 1985) under the condition of small duty cycles $[T_{on}/(T_{on} + T_{off})]$, although its validity for larger duty cycles is questionable. Ibl's model provides an instant grasp of the physical phenomena of the complicated pulse plating process as well as a simple way to calculate the concentration profile. However, the model is limited to single metal deposition with no consideration of the kinetics of the associated electrode reaction.

These analytical approaches have given us a picture of the pulse plating process; however, they are limited to special cases. The concept of a pulse-limiting current density, i_{pg}, as presented in these analytical treatments, loses its usefulness when the more practical case of multiple electrode reactions of pulse alloy plating is considered. This is true because when multiple electrode reactions occur no single reaction can be kept at a constant rate during the pulse. The electrode potential will rise in such a way as to adjust the relative reaction rates to accommodate to the total applied current density, i_p. Although for single reactions the rate of any nondirect current method cannot exceed the direct current electrolysis (Cheh, 1971), Viswanathan et al. (1980) pointed out that, for multiple reactions, the rates of less

kinetically favored reactions can be enhanced by using a current pulse. Thus, one would expect that the selectivity for less noble species in the deposited alloy could be increased by adjusting the pulse parameters. In order to quantitatively investigate the influence of pulse parameters on the selectivity and current efficiency of the electrodeposition of alloys, a more complete model than these analytical models is needed. This model should include rate expressions for the electrode reactions.

More complete models than the analytical models have been presented. For example, Popov et al. (1976) proposed a potential controlled pulse plating model for copper deposition and solved the equations using finite differences. This model includes a rate expression at the surface, but it is restricted to single metal with diffusion as the only mode of mass transport. In addition, they used the common assumption that the applied potential is equal to the electrode overpotential. This assumption is questionable because the applied potential is actually the potential difference between the working electrode and a reference electrode placed in the solution near the working electrode. This potential difference includes the electrode overpotential and solution ohmic drop, which in many cases can be important.

Another example of a more complete model is that of Fedkiw and Brouns (1988). They solved the potential controlled pulse deposition of a single metal on a planar electrode. Unfortunately, they made the same assumption about the applied potential as that made by Popov et al. Pesco and Cheh (1988) simulated the electrodeposition of a Sn-Pb alloy on a rotating disk electrode (RDE). In their work, they used another common assumption (eg., White and Newman, 1977) that is only approximately correct. They assumed that Laplace's equation governs the potential distribution within the bulk solution near the RDE and within the thin diffusion layer on the RDE. As shown by White et al. (1977), the potential at an electrode as predicted by Laplace's equation can be significantly different from that predicted by using dilute solution theory including the effect of ionic migration. This is important because the predicted current density depends exponentially on the potential difference between the electrode and the adjacent solution. Verbrugge and Tobias (1985, 1988) calculated the periodic electrodeposition of alloys on a RDE with the consideration of solid-phase component interaction. They did this by introducing a set of equations that describe the solid-phase thermodynamic equilibrium. Unfortunately, migrational mass transport was neglected in their calculations. A similar superposition method was employed by Ruffoni and Landolt (1988) when they simulated Au-Cu-Cd pulse plating under diffusion-only conditions. Recent publications on galvanostatic and potentiostatic pulse electrolysis have also been presented by Wan and Cheh (1988). They used the orthogonal collocation method to solve the equations for copper deposition on a RDE. They made essentially the same assumption as those made by Pesco and Cheh (1988).

In the model presented here, the effect of migration is considered and any pulse form can be applied by using an explicit expression, as shown in the model development section. The electrodeposition of Ni-Cr with a square current pulse is used for illustration. The model can be used to predict deposit thickness and alloy composition profiles as well as other quantities such as current efficiency.

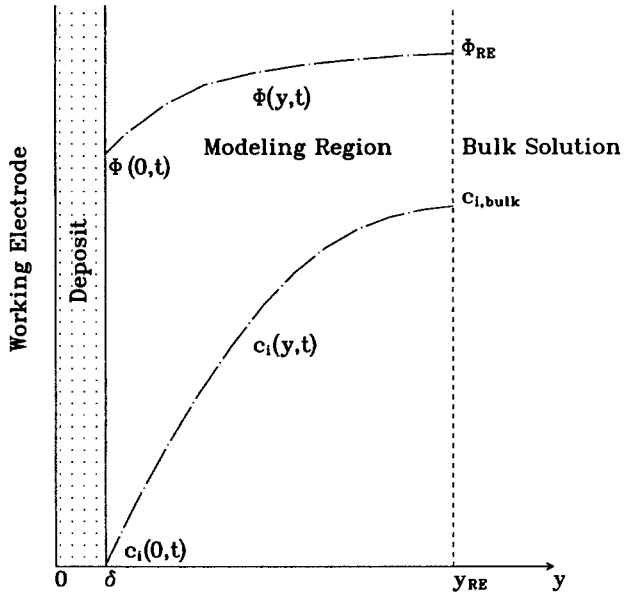

Figure 1. The region modeled.

The solution potential and concentration profiles are shown here for illustration only. They do not represent any particular deposition process.

Model Development

A one-spatial-coordinate model is used, which assumes the current density distribution to be uniform on the surface of a RDE. This assumption is essentially the same as that used earlier by Newman (1966, 1967). Therefore, this model is strictly valid only at the center of the electrode. It would be valuable to extend this model to include the effect of radial gradients, which was considered to be beyond the scope of this work. Additional assumptions used in the development of the model are as follows:

- Dilute solution theory applies: i.e., there is no interaction between ionic species in the solution.
- There are no homogeneous chemical reactions in the solution. This assumption can be relaxed as shown by Ying et al. (1988).
- Double-layer charging is unimportant.
- Relative activities of the solid species can be replaced by their atomic percentages.
- The solution is isothermal.
- There is no conductive resistance in the solid phase, including the interface between the working electrode and the deposited alloy.
- The alloy does not dissolve during the relaxation time: that is, the dealloying process is not incorporated to the present model.

Governing equations

The modeling region is shown schematically in Figure 1. The whole process is assumed to be controlled by a galvanostat which provides the pulse current. The dependent variables involved in the model are the species concentrations $c_i(y, t)$, the potential in the solution $\Phi(y, t)$, the deposit thickness $\delta(t)$, the compositions of the components in the alloy $x_k(t)$, and the electrode potential $V_d(t)$.

The material balance for species i in the solution is

$$\frac{\partial c_i}{\partial t} = -\nabla \cdot \mathbf{N}_i \qquad (1)$$

where N_i is the molar flux of species i. N_i includes migration, diffusion, and convection (Newman, 1973, p. 301):

$$\mathbf{N}_i = -z_i u_i \mathrm{F} c_i \nabla\Phi - D_i \nabla c_i + \boldsymbol{v} c_i \tag{2}$$

for the one-dimensional model presented here, the velocity near a RDE can be written as (Ryan et al., 1987)

$$v_y = -a\Omega\left(\frac{\Omega}{\nu}\right)^{1/2}(y - \delta)^2 \tag{3}$$

which is one-term approximation in the region close to the electrode with correction for the thickness of the deposited layer δ. Note that for a fixed point in the solution phase, the magntiude of v_y decreases with time as δ increases. Substitution of Eq. 2 into Eq. 1 yields

$$\frac{\partial c_i}{\partial t} = D_i \frac{\partial^2 c_i}{\partial y^2} - v_y \frac{\partial c_i}{\partial y} + z_i u_i \mathrm{F}\left(c_i \frac{\partial^2 \Phi}{\partial y^2} + \frac{\partial c_i}{\partial y}\frac{\partial \Phi}{\partial y}\right) \tag{4}$$

The ionic mobility u_i is assumed to be related to the diffusion coefficient D_i, according to the Nernst-Einstein equation [$u_i = D_i/(RT)$, Newman, 1973, p. 229]. To account for the potential distribution Φ, the electroneutrality condition is used:

$$\sum_{i=1}^{nion} z_i c_i = 0 \tag{5}$$

Boundary conditions

The boundary conditions at $y = \delta$ for concentrations are obtained from a component material balance at the interface. The flux for each ionic species i is equal to the sum of its reaction rates at the interface:

$$\sum_{j=1}^{nr} \frac{s_{ij} i_j}{n_j \mathrm{F}} = z_i u_i \mathrm{F} c_i \left.\frac{\partial \Phi}{\partial y}\right|_{y=\delta} + D_i \left.\frac{\partial c_i}{\partial y}\right|_{y=\delta} \tag{6}$$

where s_{ij} is the stoichiometric coefficient of species i in reaction j when reaction j is written as

$$\sum_i s_{ij} M_i^{z_i} \rightarrow n_j e^- \tag{7}$$

and n_j is the number of electrons transferred in reaction j. The partial current density of reaction j, i_j, is assumed to be given by the Butler-Volmer equation as presented by Chen et al. (1988).

Also, the electroneutrality condition (Eq. 5) is assumed to hold at the interface $y = \delta$.

The change of deposit thickness depends on the accumulation of all metal species at the surface and can be written as follows:

$$\frac{\partial \delta}{\partial t} = -\sum_{l=1}^{m} \frac{MW_l}{\rho_l}\left(\sum_{j=1}^{nr} \frac{s_{lj} i_j}{n_j \mathrm{F}}\right) \tag{8}$$

where MW_l and ρ_l are the molecular weight and solid density of each metal species l. The deposit composition of species k is the ratio of individual to the total deposition rate:

$$x_k = \frac{\sum_{j=1}^{nr} \frac{s_{kj} i_j}{n_j \mathrm{F}}}{\sum_{l=1}^{m}\sum_{j=1}^{nr} \frac{s_{lj} i_j}{n_j \mathrm{F}}} \tag{9}$$

The total current density $i_T(t)$, which is controlled by a galvanostat, is the sum of all of the partial current densities:

$$i_T = \sum_{j=1}^{nr} i_j \tag{10}$$

It is worth noting that any form of the applied current density could be employed; however, for simplicity a square wave current density is used below in our example. For a square wave, $i_T = i_p$ during the pulsating period, while $i_T = 0$ during the relaxation period.

The boundary conditions at $y = y_{RE}$ where the reference electrode is placed are simply

$$c_i(y_{RE}, t) = c_{i,\,\mathrm{bulk}} \tag{11}$$

where

$$\sum_{i=1}^{nion} c_{i,\,\mathrm{bulk}}\, z_i = 0,$$

and

$$\Phi(y_{RE}, t) = \text{arbitrary constant potential (e.g., 0V)} \tag{12}$$

The value of y_{RE} is larger than that for the diffusion layer thickness so that the solution at $y = y_{RE}$ is perfectly mixed. It should be pointed out that the value chosen for $\Phi(y_{RE},t)$ is totally irrelevant to the model results. Experimentally, neither $V_d(t)$ nor $\Phi(y_{RE},t)$ can be measured, only their difference, $V_d - \Phi_{\mathrm{RE}}$, can be measured. The potential in the solution at y_{RE} depends on the current being passed. Numerically, we arbitrarily assign a constant value for Φ_{RE} as a basis for solving for the solution potential profile, $\Phi(y,t)$, as well as the electrode potential, $V_d(t)$. A similar procedure for potentiostatic control was presented earlier by White et al. (1983).

The initial conditions can be easily visualized. Before deposition occurs, there are no concentration gradients within the solution and the total current density is zero.

Solution technique

A finite difference formulation is used to solve the above set of differential equations. The region between δ and y_{RE} is divided equally into N intervals. The total number of intervals is fixed; however, the grid size will decrease as the electrodeposition process occurs. The node numbers and positions are specified as shown in Figure 2. The total time derivative of $c_i(y,t)$ at a certain moving node P can be expressed as follows (Murray and Landis, 1959):

$$\left.\frac{dc_i}{dt}\right|_P = \left.\frac{\partial c_i}{\partial y}\right|_P \left.\frac{\partial y}{\partial t}\right|_P + \left.\frac{\partial c_i}{\partial t}\right|_P \tag{13}$$

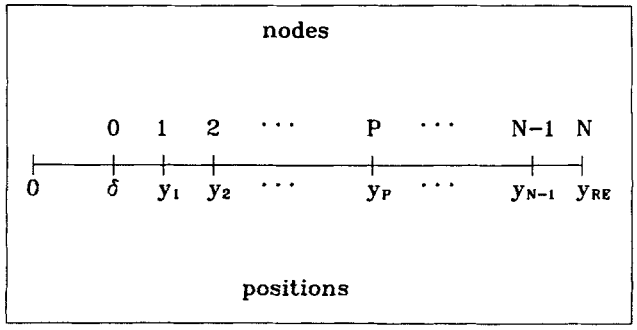

Figure 2. Positions of moving nodes at a particular time.

After algebraic manipulation according to the geometric relationship of node P in Figure 2, one obtains

$$\left.\frac{\partial y}{\partial t}\right|_P = \frac{N-P}{N}\frac{\partial \delta}{\partial t} \tag{14}$$

Substituting Eqs. 13 and 14 into Eq. 4 yields

$$\left.\frac{dc_i}{dt}\right|_P - \frac{N-P}{N}\frac{\partial c_i}{\partial y}\left|_P \frac{\partial \delta}{\partial t} - D_i\frac{\partial^2 c_i}{\partial y^2}\right. + v_y\frac{\partial c_i}{\partial y} - z_i u_i \mathrm{F}\left(c_i\frac{\partial^2 \Phi}{\partial y^2} + \frac{\partial c_i}{\partial y}\frac{\partial \Phi}{\partial y}\right) = 0 \tag{15}$$

Since the governing equations and boundary conditions should be expressed in the finite difference form, a new variable appears, i.e., the grid size $\Delta y(t)$, which becomes smaller with time as the deposited alloy layer grows. To account for this new variable, another equation (Nguyen, 1988) is written as

$$\Delta y = \frac{y_{RE} - \delta}{N} \tag{16}$$

All of the terms that contain derivatives with respect to y are expressed by a three-point finite difference approximation. In the solution phase, a central difference approximation is used; at the boundaries $y = \delta$ and $y = y_{RE}$, three-point forward and backward approximations are used, respectively. Alternatively, the variable Δy can be eliminated by substituting Eq. 16 into the finite difference version of Eq. 15. However, this was not done because of the tedious algebra. The structure of the governing equations and related boundary conditions is presented in Table 1. Note that Eq. 16 is used as a boundary condition at $y = \delta$. As shown in Table 1, the values c_i and Φ are distributed over the whole region $\delta \le y \le y_{RE}$, while δ, x_k, V_d, and Δy have only single values which are determined by the boundary conditions at $y = \delta$. The entire set of equations is solved by using Newman's BAND(J) subroutine (Newman, p. 414, 1973) with an implicit time-stepping technique to solve the pulse-plating problem. This method includes an iterative procedure known as the Newton-Raphson (NR) method at each time step. One numerical convenience should be addressed here. Because of the solution method used in BAND(J), each variable needs to be described by an algebraic equation at each node. To accommodate this, a constant variable approach (White et al., 1977; Nguyen, 1988; Chen et al., 1988) was used:

$$\frac{\partial w}{\partial y} = 0 \tag{17}$$

where w stands for variable δ, x_k, V_d, or Δy.

Table 1. Equations Used

Variables	Governing Eqs. $\delta < y < y_{RE}$	Boundary Conditions $y = \delta$	Boundary Conditions $y = y_{RE}$
c_i	15	6	11
Φ	5	5	12*
δ	17**	8	17**
x_k	17**	9	17**
V_d	17**	10	17**
Δy	17**	16	17**

*As discussed in the model development section, the value given for Φ at y_{RE} is totally arbitrary, which only serves as a basis for the calculation of the potential profile. Refer to White et al. (1983) for more detail.

**The variables δ, x_k, V_d, and Δy are represented by w in Eq. 17.

Table 2. Electrochemical Reactions

Reaction j	Expression	U_j^{θ}* (V)
1	$Cr^{+3} + e^- \rightarrow Cr^{+2}$	−0.41
2	$Cr^{+2} + 2e^- \rightarrow Cr$	−0.557
3	$Ni^{+2} + 2e^- \rightarrow Ni$	−0.23
4	$2H^+ + 2e^- \rightarrow H_2$	0.0

*Taken from Bard and Faulkner (1980, p. 700).

Parameters

The reactants and supporting electrolyte for a chloride plating bath are as follows: $CrCl_3 \cdot 6H_2O$ (0.15 M), $NiCl_2 \cdot 6H_2O$ (0.05 M), NaCl (0.5 M), and HCl (0.05 M). They are assumed to be completely dissociated. Sodium chloride serves as the supporting electrolyte. Hydrochloric acid is added to obtain the desired low pH. The electrochemical reactions that are assumed to occur are shown in Table 2; the corresponding stoichiometric relationship and reaction orders are shown in Table 3. As shown in Table 2, Cr^{+3} is reduced to Cr^{+2}, and then Cr^{+2} is reduced to Cr sequentially (Zielińska-Ignaciuk and Galus, 1974; Niki et al., 1986, p. 256). Cr^{+2} will be in a stable oxidation state in aqueous solutions if there are no oxidizing agents present such as oxygen (Niki et al., 1986, p. 256). The effect of complexing of Cr^{+3} with chloride ions was neglected in this work. This was

Table 3. Stoichiometry and Electrochemical Reaction Orders

	Reaction 1			Reaction 2			Reaction 3			Reaction 4		
Species (i)	s_{ij}	p_{ij}	q_{ij}	s_{ij}	p_{ij}	q_{ij}	s_{ij}	p_{ij}	q_{ij}	s_{ij}	p_{ij}	q_{ij}
Cr^{+3}	−1	0	1	0	0	0	0	0	0	0	0	0
Cr^{+2}	1	1	0	−1	0	1	0	0	0	0	0	0
Ni^{+2}	0	0	0	0	0	0	−1	0	1	0	0	0
H^+	0	0	0	0	0	0	0	0	0	−2	0	2
Na^+	0	0	0	0	0	0	0	0	0	0	0	0
Cl^-	0	0	0	0	0	0	0	0	0	0	0	0
Metal (k)	s_{kj}	p_{kj}	q_{kj}	s_{kj}	p_{kj}	q_{kj}	s_{kj}	p_{kj}	q_{kj}	s_{kj}	p_{kj}	q_{kj}
Cr	0	0	0	1	1	0	0	0	0	0	0	0
Ni	0	0	0	0	0	0	1	1	0	0	0	0

Table 4. Kinetic Parameters

Reactions j	α_{ij}	α_{cj}	n_j	$i^*_{oj,\mathrm{ref}}$(A/cm^2)
1	0.45	0.55	1	9.16×10^{-3}**
2	0.86	1.14	2	2.7×10^{-3}**
3	0.8	1.2	2	1.07×10^{-8}†
4	1.0	1.0	2	6.3×10^{-6}‡

*Calculated from literature values corrected to the specified reference concentrations in Table 4 using an expression $i_{oj,\mathrm{ref}} = i_{oj,\mathrm{data}} \Pi_i (c_{i,\mathrm{ref}}/c_{i,\mathrm{data}})^{\gamma ij}$, where the subscript *data* are used to represent the literature data.
**Niki et al. (1986, pp. 355, 349).
†Tamamushi (1975, p. 91).
‡Bockris and Reddy (1970, p. 1238).

done because the data of Baltisberger and King (1964) can be extrapolated to 25°C to obtain a value of 0.082 L/mol for the stability constant for the reaction $Cr^{+3} + Cl^- \rightarrow CrCl^{+2}$. Thus, the concentration of $CrCl^{+2}$ would be only about 8% of the concentration of Cr^{+3}. It would be possible to include this easily in the model, if desired (e.g., Ying et al., 1988). In addition, the effect of complexing of Ni^{+2} by Cl^- was ignored because it is not certain that this complexing occurs. That is, NBS data (Zemaitis et al., 1986, p. 449) indicate that no complexing occurs whereas the data by Russian workers does indicate complexing of Ni^{+2} by Cl . Until additional data are available, it seems reasonable to neglect this effect.

The kinetic parameters and operating conditions are shown in Tables 4 and 5. The reference concentration for each species, $c_{i,ref}$, is chosen to be 1 M for convenience. Note that the corresponding $i_{oj,ref}$ in Table 4 was calculated based on the reference concentrations because $c_{Cr^{+2},\mathrm{bulk}}$ is equal to zero.

The discussions in the next section are based mainly on a typical square wave with $i_p = -0.3$ A/cm^2, while the pulse period and the relaxation period are both set 50 ms, i.e., 100 ms cycle time with duty cycle $\gamma = 0.5$.

Results and Discussions

Model results

Figure 3 shows a simulated direct current *d–c* polarization curve and the partial current densities for each reaction. This was done by using the *d–c* version of the model presented here (see Chen et al., 1988) with the operating conditions shown in

Table 5. Reacting Species and Operating Conditions

Ionic Species	Cr^{+3}	Cr^{+2}	Ni^{+2}	H^+	Na^+	Cl^-
$c^*_{i,\mathrm{ref}}$(M)	1.0	1.0	1.0	1.0		
$c_{i,\mathrm{bulk}}$(M)	0.15	0.0	0.05	0.05	0.5	1.1
D_i(cm^2/s) · 10^5	0.595**	0.732***	0.666**	0.931†	1.334†	2.032†
Metal	Cr	Ni				
$a^*_{k,ref}$	1	1				
ρ_l(g/cm^3)	7.20‡	8.902§				
MW_l(g/mol)	51.996	58.7				

$T = 298.15$ K $\Omega = 104.7$ rad/s $\rho_o = 1$ g/cm^3
$\nu = 0.0123$ cm^2/s $y_{RE} = 0.02$ cm

*Chosen arbitrarily for convenience.
**Calculated from the equivalent conductance (λ) in Dean (1985, pp. 6–34).
***Calculated by using λ = 55 mho · cm^2/equivalent.
†Taken from Newman (1973, p. 230).
‡Chosen from Weast (1981, p. B-12).
§Chosen from Weast (1981, p. B-27).

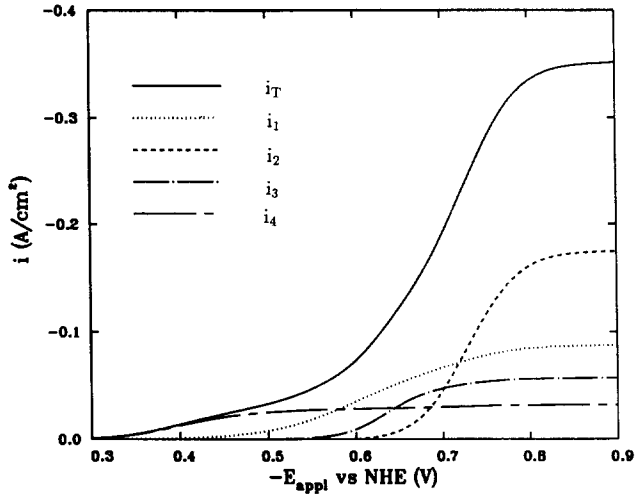

Figure 3. Simulated direct current polarization curve for Ni-Cr alloy electrodeposition.

Table 5. Due to the low exchange current densities used for reactions 3 and 4, hydrogen evolution and nickel deposition will not occur until $-E_{appl}$ is greater than 0.3 V and 0.55 V, respectively. The deposition of Cr begins at about 0.6 V, and goes through a larger Tafel region than that for Ni and then reaches a current density plateau region. Clearly, the codeposition of Ni and Cr occurs in a potential region where Ni is at its limiting current while Cr is in a kinetically controlled region; they have an intersection at about 0.7 V. The plateau for reaction 2 should not be viewed as the normal limiting current. Rather, it is a balance between the electrode reactions and the transport of Cr^{+2} away from the electrode surface. The simulated *d–c* polarization curve shown in Figure 3 is presented to help understand the dynamic behavior of pulse plating.

Simulated partial current density profiles are shown in Figure 4. After two or three cycle times, the process appears to become one with a periodic steady state. Considering the fourth cycle, for example, shows that reactions 1 and 3 quickly pass through a maximum after four to seven ms then drop, while reaction 2 starts with a finite value and picks up steadily to the end of the pulse. The hydrogen evolution (reaction 4) drops rapidly at the

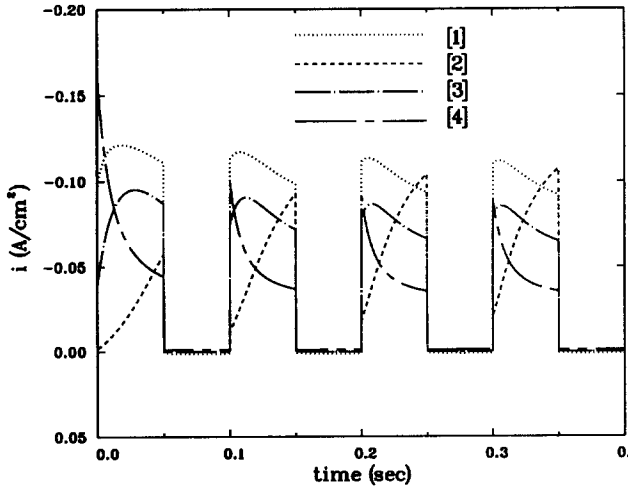

Figure 4. Partial current density profiles.

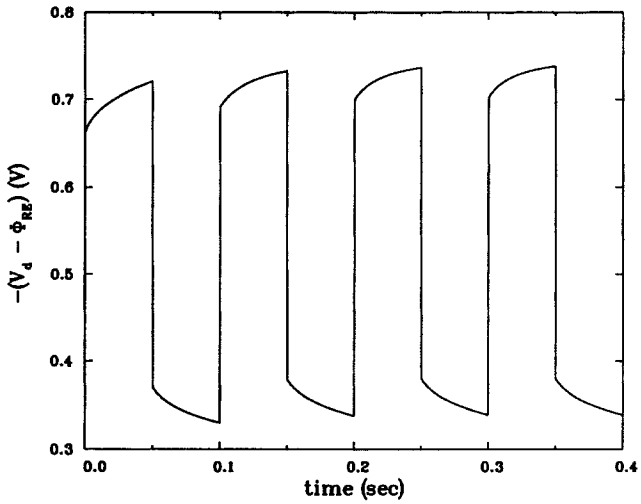

Figure 5. Potential response.

onset of T_{on} and then arrives at a smooth region near the end of T_{on}. This behavior can be understood better by considering the variation of the potential difference between V_d and Φ_{RE}, as shown in Figure 5. For Cr^{+3} and Ni^{+2}, the initial rise of the potential indeed favors reactions 1 and 3, but the insufficient mass transfer of these two species from the bulk causes the current density to drop. Thus, a hump results in the partial current density profiles. These humps appear to be more significant during the initial transient pulse period. This is easy to comprehend if one remembers that before deposition the bulk concentrations also prevail to the electrode surface; therefore, for the first pulse the reactants will take longer time to be depleted. The potential rise and the concentration depletion determine the position of the hump in the partial current density profiles. Note that Figure 5 also shows the smaller initial overall potential response ($-0.66 \sim -0.72$ V) in comparison with the periodic steady-state values (over -0.7 V).

Figure 6 shows the composition profiles of the alloy. These are basically parallel to the partial current density profiles in Figure 4. The decrease of the slope for the chromium composition after the first pulse indicates the role of mass transfer limitation. That

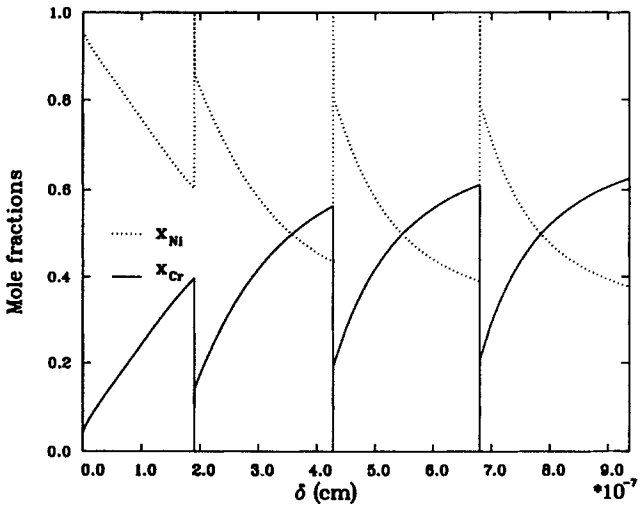

Figure 6. Composition profiles.

$\bar{x}_{Cr} = 0.4961$, $\bar{x}_{Ni} = 0.5039$ at periodic steady state.

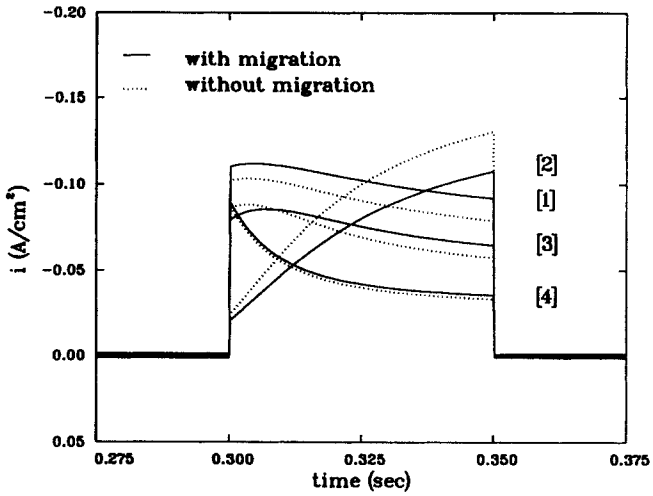

Figure 7. Migration effect on partial current densities.

$T_{on} = 50$ ms, $T_{off} = 50$ ms, $i_p = -0.3$ A/cm^2. Bulk concentration is chosen as that in Table 5.

is, although Cr^{+2} is generated at the interface, the diffusion of Cr^{+2} away from the electrode during T_{on} slows down the increase of reaction 2. The periodic composition profiles are quite common in current controlled processes (Cohen et al., 1983; Despić and Jović, 1987).

Migration effect

Figure 7 shows partial current densities without considering migration in comparison with those including migration. The migration-excluded case was obtained by modifying the complete model. This was done by removing the solution potential related terms (i.e., those containing $\partial\Phi/\partial y$ or $\partial^2\Phi/\partial y^2$) from the model equations (Eqs. 4, 6 and 15). Once this was done, the electroneutrality condition (Eq. 5) was no longer needed. The problem was then solved again using the same applied current density to obtain the dotted lines in Figure 7. The solution ohmic drop ($\Phi_o - \Phi_{RE}$) for the without-migration case can be approximated by $|i_T| \cdot (1/\kappa) \cdot (y_{RE} - \delta)$, where the solution conductivity $\kappa = F^2 \Sigma_{i=1}^{nion} z_i^2 u_i C_{i,\,bulk}$ (Newman, 1973, p. 221). Another way to calculate the without-migration case would be to set the mobilities of all of the reactants equal to zero and assume that all of the current is carried by the sodium and chloride ions, as suggested by a reviewer of this paper. In this case, the electroneutrality equation with all charged species included would be used to determine the distribution of the potential in the solution. This approach would provide a direct method of calculating the ohmic drop at the same time as the partial current densities are calculated, but the predicted ohmic drop would be too large because the conductivity of the plating solution is greater than that of a solution of sodium chloride. In other words, the reacting species also carry the current. The most important point is that the predicted partial current densities are the same for both of these without-migration cases. The reason for this is that the partial current densities depend on the total applied current density and not on the ohmic drop.

As shown in Figure 7, the current densities for reactions 1, 3 and 4 for the case without the effect of migration-included are lower than their migration-included counterparts; however, the current density for the reaction that accounts for the deposition of chrome increases significantly. The deviation between these

two cases increases along with the pulse period. It is clear that in the current controlled pulse plating of alloys, such migration effect may change the relative rates of the reactions and thus alter the composition of the alloy.

The surface overpotential response, $-(V_d - \Phi_o)$, shown in Figure 8 is used to demonstrate the effect due to migration. Due to the missing of migrational transport for species Cr^{+3}, Ni^{+2}, and H^+ in the migration-excluded case, the electrode overpotential increases in such a way as to enhance the rate of reaction 2 to accommodate to the total applied current density ($i_p = -0.3$ A/cm^2). On the other hand, one may say that the enhanced mass transfer due to the migration effect was offsetted by the less available surface overpotential. As the potential rises along the pulse period, the rate of the more kinetic-sensitive reaction (Eq. 2) increases, at the expense of the decreased rates of Eqs. 1, 3 and 4, those suffered from concentration depletion (mass transfer from the bulk is not fast enough to maintain the reaction rates). This explains why a higher chrome composition is predicted when not considering migration, because a larger electrode overpotential is available. Thus, in the current-controlled electrodeposition process, the significance of the effect of migration is shown by the competing rates among the individual reactions.

Figure 9 depicts the concentration profiles for the reactants between these two cases at the end of a pulse under the periodic steady state. The profiles for supporting electrolytes Na^+, Cl^- are not shown. The dimensionless distance ζ is calculated by $(y - \delta)/\hat{\delta}$, where the diffusion layer thickness is $\hat{\delta}$ is defined (White et al., 1977):

$$\hat{\delta} = \left(\frac{3D_R}{a\nu}\right)^{1/3} \left(\frac{\nu}{\Omega}\right)^{1/2} \tag{18}$$

where D_R is the diffusion coefficient of the limiting reactant, which is H^+ here. It is clear that the electric field pushes the concentrations of positive ions closer to the electrode which enhances the mass transfer of Cr^{+3}, Ni^{+2} and H^+ by migration. The influence of migration depends on the charges of ionic species, their diffusion coefficients, and the magnitude of the potential gradient in the system. The change in concentration gradients in Figure 9 indicates that migration also indirectly

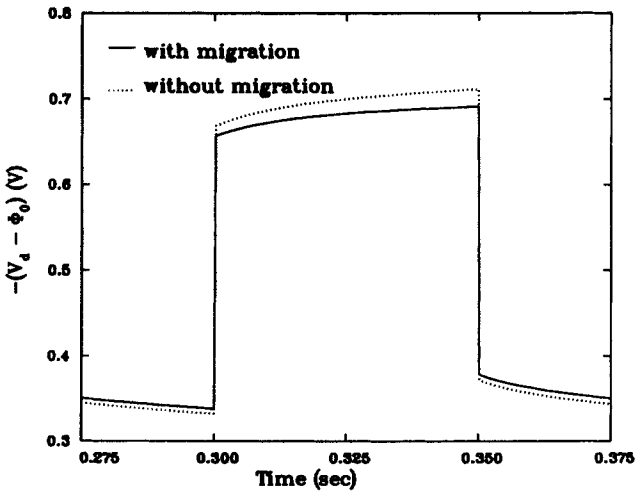

Figure 8. Comparison of electrode overpotential with and without migration effect.

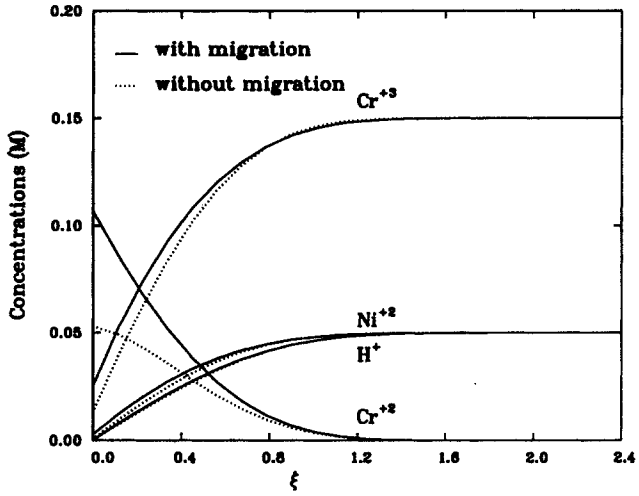

Figure 9. Effect of migration on the concentration profiles at the end of pulsating time.
Dimensionless distance ξ is defined as $(y - \delta)/\hat{\delta}$.

influences the diffusion mechanism. Note that, for the intermediate species Cr^{+2}, the direction of migration is opposite to that of diffusion because Cr^{+2} is produced at the electrode surface. The interface concentration of Cr^{+2} is the balance between the generation rate by reaction 1, the coupled effects of reaction 2, and the mass transfer of Cr^{+2} away from the electrode. For the case without migration, the higher available electrode overpotential, which favors reaction 2, will induce a lower Cr^{+2} concentration at the interface and, in turn, less diffusion away from the surface.

Current efficiency and selectivity

Figure 10 shows the alloy current efficiency as defined:

$$\theta_{p\text{-}c} = \frac{\int_{\text{one cycle}} (1.5i_2 + i_3)\, dt}{i_p T_{\text{on}}} \tag{19}$$

The factor 1.5 is used because each Cr^{+2} is reduced due to the

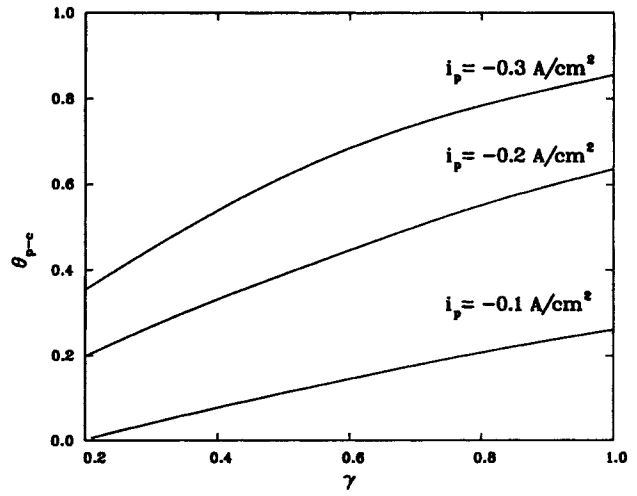

Figure 10. Current efficiency of alloy at different duty cycle.
T_{off} = 50 ms.

consumption of one Cr^{+3} from the bulk. It is clear from Figure 10 that a higher current efficiency is obtained at larger duty cycles and higher pulse current densities. Because under these conditions, the relatively less kinetically favored reactions (Eqs. 2 and 3; see Figure 3) will increase along the potential rise at the expense of the sudden depletion of H^+. A larger applied current density helps the potential shift to the region that favors metal deposition. For the case of $i_p = -0.1$ A/cm^2, most of the current was consumed by hydrogen evolution and the reduction of Cr^{+3}. The increase of θ_{p-c} is reduced as i_p rises from -0.2 to -0.3 A/cm^2, which indicates that the limitation of mass transfer on metal deposition also occurs at higher i_p. It should be noted that the dealloying of Cr during the rest period is not considered here. This assumption should be reasonable because Cr is easily passivated during the anodic process (McBee and Kruger, 1972; Kawashima et al., 1984; Archer et al., 1987).

The average solid-phase composition for Cr, $\bar{x}_{Cr}$, is shown in Figure 11 and can be viewed as the selectivity for Cr. It is calculated as follows:

$$\bar{x}_{Cr} = \frac{1}{\Delta\delta} \int_{\text{one cycle}} x_{Cr}\, d\delta \tag{20}$$

where $\Delta\delta$ is the increase of deposit thickness for one cycle. It is not surprising that $\bar{x}_{Cr}$ has the same trend as that of θ_{p-c}. The increase of the deposition rate of Cr at higher pulse current densities and larger duty cycles induces higher electrode overpotentials; consequently, it accounts for both the higher current efficiency and the higher Cr selectivity. On the other hand, a lower pulse current density and a smaller duty cycle would favor higher Ni composition (selectivity of Ni would be better) but a lower alloy current efficiency.

Figure 12 shows a comparison between the current efficiency for p–c and d–c. The following definition is employed:

$$\text{relative current efficiency} = \left.\frac{\theta_{p-c}}{\theta_{d-c}}\right|_{i_p\gamma = i_{d-c}} \tag{21}$$

where $\theta_{d-c} = (1.5\, i_2 + i_3)/i_{d-c}$ under direct current condition, and θ_{d-c} is obtained with the same code by using a large enough

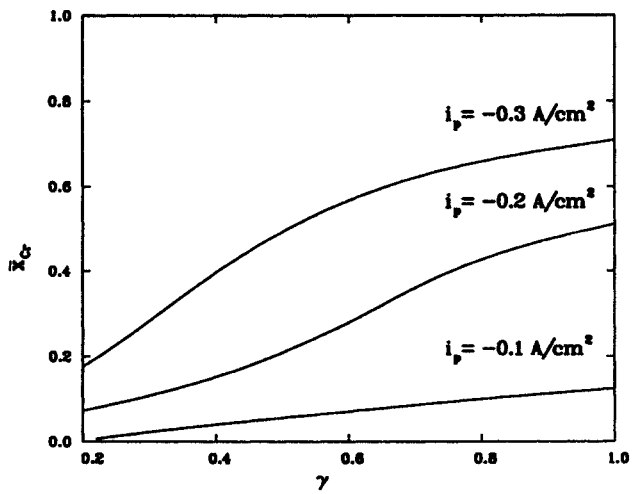

Figure 11. Selectivity of Cr at different duty cycle.
T_{off} = 50 ms.

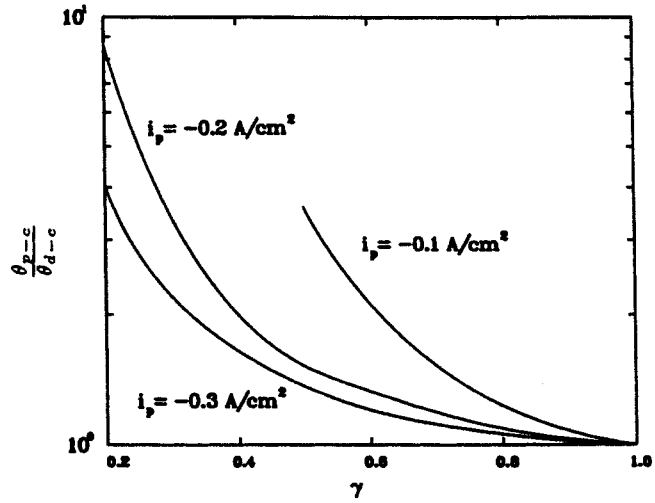

Figure 12. Relative current efficiency of p–c to d–c plating.

value for T_{on} so that all the partial current densities reach their d–c steady-state values under a specified applied current density. The relative current efficiency is calculated based on the same amount of charge: i.e., $i_p\gamma = i_{d-c}$. Note that $\gamma = 1$ is the limiting case for p–c with an infinite pulse time, which is equivalent to d–c. Obviously, pulse plating has a much better current efficiency than d–c plating. The deviation between the two processes becomes more significant at low pulse current densities and small duty cycles because at these conditions the d–c is almost dominated by hydrogen evolution. The relative selectivity of chrome, which is not shown here, has in the same trend as that of the relative current efficiency but is even more sensitive to the duty cycle.

Conclusion

A general pulse plating model for the electrodeposition of alloys is presented. The model is illustrated by considering the electrodeposition of Ni-Cr. The relative rates of the multiple reactions with different pulse parameters are governed by the interplay between electrode kinetics and mass transport. The effect of migration is an important factor that should be included when predicting the relative reaction rates for a galvanostatic process. For the plating process considered here, hydrogen evolution is reduced by using pulse current plating relative to direct current plating. The deposition rates of Cr and the alloy current efficiency are also enhanced by using pulsating current.

Acknowledgment

The authors are grateful for the support of this project given by the Sandia National Laboratories, the Texas Advanced Technology and Research Program, and the Texas A&M University Board of Regents through the Available University Fund.

Notation

a = 0.51023
$a_{k,ref}$ = reference relative activity of metal k in the deposit
c_i = concentration of species i, mol/cm^3
$c_{i,bulk}$ = bulk solution concentration of species i, mol/cm^3
$c_{i,data}$ = literature concentration of species i that correspond to $i_{oj,data}$, mol/cm^3
$c_{i,ref}$ = reference concentration of species i, mol/cm^3

D_i = diffusion coefficient of species i, cm^2/s
D_R = diffusion coefficient of the diffusion controlling species, cm^2/s
E_{appl} = applied potential ($=V_d - \Phi_{RE}$), V
F = Faraday's constant, 96,487 C/mol
i_j = partial current density due to reaction j, A/cm^2
i_{lim} = limiting current density of direct current, A/cm^2
$i_{oj,data}$ = exchange current density data from literature, A/cm^2
$i_{oj,ref}$ = exchange current density at reference concentrations for reaction j, A/cm^2
i_p = pulse current density, A/cm^2
i_{pg} = pulse limiting current density, A/cm^2
i_T = total current density, A/cm^2
MW_l = molecular weight of solid component l, g/mol
m = number of solid species
$nion$ = number of ionic species
n_j = number of electrons transferred in reaction j
N_i = flux vector of species i, $mol/cm^2 \cdot s$
nr = number of electrochemical reactions
p_{ij} = anodic reaction order of ionic species i in reaction j
p_{kj} = anodic reaction order of solid component k in reaction j
q_{ij} = cathodic reaction order of ionic species i in reaction j
q_{kj} = cathodic reaction order of solid component k in reaction j
R = universal gas constant, 8.3143 J/mol · K
s_{ij} = stoichiometric coefficient of ionic species i in reaction j
s_{kj} = stoichiometric coefficient of solid component k in reaction j
T = absolute temperature, K
T_{on} = pulse time, ms
T_{off} = relaxation time, ms
u_i = mobility of species i [it is assumed here that $u_i = D_i/(RT)$], $mol \cdot cm^2/J \cdot s$
U_j^θ = standard electrode potential for reaction j, V
$\boldsymbol{v}$ = electrolyte velocity vector, cm/s
v_y = electrolyte velocity in the normal direction, cm/s
V_d = potential of the working electrode, V
w = stands for δ, x_k, V_d, or Δy in Eq. 17
x_k = mole fraction of metallic species k in the electrodeposit
$\bar{x}_{Cr}$ = averaged mole fraction of Cr in the electrodeposit
$\bar{x}_{Ni}$ = averaged mole fraction of Ni in the electrodeposit
y = normal coordinate, cm
y_{RE} = position of reference electrode, cm
z_i = charge number of species i

Greek letters

α_{aj} = anodic transfer coefficient for reaction j
α_{cj} = cathodic transfer coefficient for reaction j
γ = duty cycle of pulse current [$=T_{on}/(T_{on} + T_{off})$]
γ_{ij} = exponent in composition dependence of exchange current density on ionic species i
δ = deposit thickness, cm
$\hat{\delta}$ = diffusion layer thickness, cm
$\Delta\delta$ = increase of deposit thickness in one cycle, cm
κ = solution conductivity, 1/ohm · cm
θ_{d-c} = current efficiency of alloy for direct current
θ_{p-c} = current efficiency of alloy for pulse current
λ = equivalent ionic conductance, mho · cm^2/equivalent
ν = kinematic viscosity, cm^2/s
ξ = dimensionless distance
ρ_l = metal density of species l, g/cm^3
ρ_o = pure solvent density, g/cm^3
Φ = potential in solution within diffusion layer, V
Φ_o = solution potential adjacent to electrode surface, V
Φ_{RE} = potential in the bulk solution at y_{RE}, V
Ω = disk rotation velocity, rad/s

Literature Cited

Archer, M. D., C. C. Corke, and B. H. Harji, "The Electrochemical Properties of Metallic Glasses," *Electrochimica Acta,* **32,** 13 (1987).

Baltisberger, R. J., and E. L. King, "Equilibrium and Kinetic Studies on the Reaction of Chromium (III) Ion and Chloride Ion in Methanol-Water Solutions," *J. Amer. Chem. Soc.,* **86,** 795 (1964).

Bard, A. J., and L. R. Faulkner, *Electrochemical Methods: Fundamentals and Applications,* Wiley, New York (1980).

Bockris, J. O'M., and A. K. N. Reddy, *Modern Electrochemistry,* Plenum Press, New York (1970).

Cheh, H. Y., "Electrodeposition of Gold by Pulsed Current," *J. Electrochem. Soc.,* **118,** 1132 (1971).

Chen, S., K.-M. Yin, and R. E. White, "A Mathematical Model for the Electrodeposition of Alloys on a Rotating Disk Electrode," *J. Electrochem. Soc.,* **135,** 2193 (1988).

Chin, D-T., "Mass Transfer and Current-Potential Relation in Pulse Electrolysis," *J. Electrochem. Soc.,* **130,** 1657 (1983).

Cohen, U., F. B. Koch, and R. Sard, "Electroplating of Cyclic Multilayered Alloy (CMA) Coatings," *J. Electrochem. Soc.,* **130,** 1987 (1983).

Datta, M., and D. Landolt, "Experimental Investigation of Mass Transport in Pulse Plating," *Surface Technol.,* **25,** 97 (1985).

Dean, J. A., *Lange's Handbook of Chemistry,* 13 ed., McGraw-Hill, New York (1985).

Despić, A. R., and V. D. Jović, "Electrochemical Formation of Laminar Deposits of Controlled Structure and Composition: I. Single Current Pulse Galvanostatic Technique," *J. Electrochem. Soc.,* **134,** 3004 (1987).

Fedkiw, P. S., and D. R. Brouns, "Periodic Electrodeposition on a Planar Electrode," *J. Electrochem. Soc.,* **135,** 346 (1988).

Ibl, N., "Some Theoretical Aspects of Pulse Electrolysis," *Surface Technol.,* **10,** 81 (1980).

Ibl, N., J. Cl. Puippe, and H. Angerer, "Electrocrystallization in Pulse Electrolysis," *Surface Technol.,* **6,** 287 (1978).

Kawashima, A., K. Asami, and K. Hashimoto, "An XPS Study of Anodic Behavior of Amorphous Nickel-Phosphorus Alloys Containing Chromium, Molybdeum or Tungsten in 1 M HCl," *Corrosion Sci.,* **24,** 807 (1984).

Marathe, V., and J. S. Newman, "Current Distribution on a Rotating Disk Electrode," *J. Electrochem. Soc.,* **116,** 1704 (1969).

McBee, C. L., and J. Kruger, "Nature of Passive Films on Iron-Chromium Alloys," *Electrochimica Acta,* **17,** 1337 (1972).

Murray, W. D., and F. Landis, "Numerical and Machine Solutions of Transient Heat-Conduction Problems Involving Melting or Freezing: I. Method of Analysis and Simple Solutions," *J. Heat Transfer, Trans. ASME,* **81,** 106 (1959).

Newman, J., "Effect of Ionic Migration on Limiting Currents," *Ind. and Eng. Chemistry Fundam.,* **5,** 525 (1966).

———, "The Effect of Migration in Laminar Diffusion Layers," *Int. J. of Heat and Mass Transfer,* **10,** 983 (1967).

Newman, J. S., *Electrochemical Systems,* Prentice Hall, Englewood Cliffs, NJ (1973).

Nguyen, T. V., private communication (1988).

Niki, K., N. Tanaka, A. Yamada, E. Itabashi, and W. H. Hartford, *Encyclopedia of Electrochemistry of the Elements,* A. J. Bard, ed., Vol. IX, Part B (1986).

Pesco, A. M., and H. Y. Cheh, "Current and Composition Distributions during the Deposition of Tin-Lead Alloys on a Rotating Disk Electrode," *J. Electrochem. Soc.,* **135,** 1722 (1988).

Popov, K. I., D. N. Keča, S. I. Vidojković, B. J. Lazarević, and V. B. Milojković, "Mathematical Model and Digital Simulation of Pulsating Overpotential Copper Electrodeposition," *J. of Appl. Electrochem.,* **6,** 365 (1976).

Rosebrugh, T. R., and W. L. Miller, "Mathematical Theory of the Changes of Concentration at the Electrode, Brought about by Diffusion and by Chemical Reaction," *J. of Phys. Chemistry,* **14,** 816 (1910).

Ruffoni, A., and D. Landolt, "Pulse-Plating of Au-Cu-Cd Alloys: II. Theoretical Modelling of Alloy Composition," *Electrochimica Acta,* **33,** 1281 (1988).

Ryan, W. E., R. E. White, and S. L. Kelly, "A Mathematical Model for the Initial Corrosion Rate of a Porous Layer on a Rotating Disk Electrode," *J. Electrochem. Soc.,* **134,** 2154 (1987).

Tamamushi, R., *Kinetic Parameters of Electrode Reactions of Metallic Compounds,* Butterworth, London (1975).

Verbrugge, M. W., and C. W. Tobias, "A Mathematical Model for the Periodic Electrodeposition of Multicomponent Alloys," *J. Electrochem. Soc.,* **132,** 1298 (1985).

Verbrugge, M. W., and C. W. Tobias, "The Periodic, Electrochemical Codeposition of Cadmium and Tellurium," *AIChE J.,* **33,** 628 (1987).

Viswanathan, K., M. A. Farrell Epstein, and H. Y. Cheh, "Simulta-

neous Discharge of Two Reacting Species under Pulse Current Conditions," *J. Electrochem. Soc.*, **127**, 2383 (1980).

Wan, H. H., and H. Y. Cheh, "The Current Distribution on a Rotating Disk Electrode in Galvanostatic Pulsed Electrolysis," *J. Electrochem. Soc.*, **135**, 643 (1988).

———, "The Current Distribution on a Rotating Disk Electrode in Potentiostatic Pulsed Electrolysis," *J. Electrochem. Soc.*, **135**, 658 (1988).

Weast, R. C., *CRC Handbook of Chemistry and Physics*, 62nd ed. (1981).

White, R. E., S. E. Lorimer, and R. Darby, "Prediction of the Current Density at an Electrode at Which Multiple Electrode Reactions Occur under Potentiostatic Control," *J. Electrochem. Soc.*, **130**, 1123 (1983).

White, R. E., and J. S. Newman, "Simultaneous Reactions on a Rotating-Disk Electrode," *J. Electroanal. Chem.*, **82**, 173 (1977).

White, R. E., J. A. Trainham, J. S. Newman, and T. W. Chapman, "Potential-Selective Deposition of Copper from Chloride Solutions Containing Iron," *J. Electrochem. Soc.*, **124**, 671 (1977).

Ying, R. Y., P. K. Ng, Z. Mao, and R. E. White, "Electrodeposition of Copper-Nickel Alloys from Citrate Solutions on a Rotating Disk Electrode: II. Mathematical Modeling," *J. Electrochem. Soc.*, **135**, 2964 (1988).

Zemaitis, J. F., D. M. Clark, M. Rafal, and N. C. Scrivner, *Handbook of Aqueous Electrolyte Thermodynamics*, AIChE, New York (1986).

Zielińska-Ignaciuk, M., and Z. Galus, "Kinetics and Mechanism of the Cr^{3+}/Cr^{2+} Electrode Reaction in Concentrated Perchlorates and Chlorides," *J. Electroanalytical Chemistry and Interf. Electrochem.*, **50**, 41 (1974).

Manuscript received Mar. 13, 1989, and revision received Nov. 21, 1989.